Effects of radical scavengers on aqueous solutions exposed to heavy-ion irradiation using the liquid microjet technique

Shinji Nomura[a], Hidetsugu Tsuchida[a,b,*], Ryousuke Furuya[a],

Kento Miyahara[a], Takuya Majima[a,b], Akio Itoh[a,b]

[a]*Department of Nuclear Engineering, Kyoto University, Kyoto 615-8530, Japan*

[b]*Quantum Science and Engineering Center, Kyoto University, Uji 611-0011, Japan*

*Corresponding author: tsuchida@nucleng.kyoto-u.ac.jp

Keywords: Radical scavenger effects, Liquid materials, Fast heavy-ion irradiation

PACS codes: 34.50.Bw; 79.20.Rf

Abstract

The effects of the radical scavenger ascorbic acid on water radiolysis are studied by fast heavy-ion irradiation of aqueous solutions of ascorbic acid, using the liquid microjet technique under vacuum. To understand the reaction mechanisms of hydroxyl radicals in aqueous solutions, we directly measure secondary ions emitted from solutions with different

ascorbic acid concentrations. The yield of hydronium secondary ions is strongly influenced by the reaction between ascorbic acid and hydroxyl radicals. From analysis using a simple model considering chemical equilibria, we determine that the upper concentration limit of ascorbic acid with a radical scavenger effect is approximately 70 μM.

1. Introduction

Investigation of the effects of ionizing radiation on liquid materials has been a major objective in radiation and nuclear sciences for many years [1]. In particular, radiolysis of liquid water is an important topic in basic research fields such as radiation chemistry, radiobiology and radiotherapy. Radiation-induced dissociation of water molecules in aqueous solutions leads to various time-dependent reactions. Namely, radiolysis processes proceed *via* three stages on respective time scales. Initially, in the physical stage ($\leq 10^{-15}$ s), ionizing radiation interacts with matter (energy transfer processes), resulting in the formation of ionized or excited water molecules (H_2O^+ and H_2O^*, respectively) and sub-excitation electrons. In the subsequent physicochemical stage (10^{-15}–10^{-12} s), free radicals (H·, OH·) and other products like hydronium ions (H_3O^+) are produced through dissociative and ion–molecular reactions. Finally, the molecular species such as molecular hydrogen (H_2) and hydrogen peroxide (H_2O_2) are formed in the chemical stage (10^{-12}–10^{-6} s). In these events, intermediate products like free radicals play an important role in the effect of radiation on

aqueous solutions.

The intermediate products are generated along the track of ionizing radiation, and the track structure (spatial distribution) depends on the type of radiation. This is known as the track effects, which are related to linear energy transfer (LET). For radiation with high LET such as high-energy heavy ions, a large amount of energy is deposited into the tracks, resulting in the formation of high concentrations of intermediate products. A variety of complicated relaxation processes then occur in the tracks during the physicochemical stage. For this reason, detailed behavior of free radicals formed in aqueous solutions by high-LET radiation is not fully understood.

The purpose of this work is to investigate the effects of radical scavengers on radiolysis of aqueous solutions by fast heavy-ion irradiation. We directly measure reaction products emitted from aqueous solutions containing radical scavengers using the vacuum liquid microjet technique combined with secondary ion mass spectrometry (SIMS) [2-4]. We use ascorbic acid ($C_6H_8O_6$) that readily reacts with OH· as a radical scavenger. A liquid target solution of ascorbic acid is irradiated by a microbeam of fast heavy ions (4.0-MeV C^{2+} ions) produced using a beam-focusing method with a tapered glass microcapillary [5]. Secondary ions emitted from the liquid surfaces are mass-to-charge analyzed with a time-of-flight (TOF) spectrometer. In this investigation, we focus on the emission yield of H_3O^+ ions that form in pairs with OH·, and its dependence on ascorbic acid concentration, providing fundamental

information about radical scavenger reactions in the physicochemical stage.

2. Experimental method

Figure 1 shows a schematic diagram of the experimental arrangement for TOF-SIMS measurement of liquid targets under vacuum by fast heavy-ion bombardments. The experimental procedures used were essentially the same as those described in our previous study [4], except for the ion-microbeam method with a capillary. Experiments were performed using a 2.0-MV Pelletron-type tandem accelerator at the Quantum Science and Engineering Center, Kyoto University. An incident projectile beam of 4.0-MeV C^{2+} ions was collimated by three sets of four-blade slits, and converted to a pulsed beam with a frequency of 40 kHz and width of 40 ns using an electrostatic beam-chopping system. The beam was directed into a tapered glass capillary with an outlet diameter (D_1) of approximately 11 μm, and focused to a spot size that matched the capillary outlet diameter. This is known as the capillary microbeam method [5]. The liquid target jet consisting of aqueous solutions of ascorbic acid was produced by effusion from a nozzle with an outlet diameter (D_2) of 24 μm at a flow rate of 0.4 mL/min using a liquid chromatography pump (Shimadzu, LC20-AD) into a collision chamber under vacuum. To maintain a high vacuum in the chamber, the jet of liquid was trapped in a liquid N_2-cooled bottle located on the bottom of the chamber.

The ion microbeam was irradiated onto the jet target as shown in Fig. 1 (a). Figure 1 (b) depicts a schematic diagram of the position of the irradiated beam on the target. The

irradiation position was adjusted using linear-motion stages moving along the X, Y and Z axes. To adjust the Z axis, we used a piezo-actuator stage to carefully change the distance (z) between the tip of the capillary and the liquid surface. The jet nozzle could be moved in the Y direction to control the irradiation position from the nozzle exit (y). In the present experiments, y and z were set to 1.0 mm and 40 μm, respectively. Making z as small as possible minimized the contribution of the irradiation beam to the vapor phase regions formed around the liquid jet. Moreover, to achieve irradiation conditions where ion beams are completely crossed with the liquid-phase regions of the jet, we monitored non-penetration of projectile ions through a jet target using a solid-state detector (SSD) located behind the jet.

Positively charged secondary ions emitted from the liquid surface were extracted perpendicularly to both the incident beam and target jet, and were mass-to-charge analyzed using a linear TOF mass spectrometer with double-stage extraction [6]. The applied electric fields in the first and second extraction regions were 0.4 and 2.0 kV/cm, respectively. After passing through a flight tube with a length L of 315 mm, the secondary ions were detected by a Channeltron detector. TOF spectra were recorded using a fast multichannel scaler (dwell time: 4 ns/channel, total number of channels per scan: 4096). To avoid neutralization of the secondary ions by collision with background gases produced from the jet, the spectrometer was equipped with a differential vacuum pumping system. The collision chamber and flight tube were separated by a small orifice with a diameter of 1.0 mm. During the operation of the

liquid jet under vacuum, the base pressure was kept below 8×10^{-2} Pa in the chamber or below 4×10^{-4} Pa in the flight tube of the spectrometer.

Aqueous solutions were prepared by mixing ascorbic acid (99.5% purity, Wako Pure Chemical Industries, Ltd.) and ultra-pure water (high-performance liquid chromatography grade, Wako Pure Chemical Industries, Ltd.). To achieve aqueous solutions of uniform concentration, the solutions were agitated continuously by a magnetic stirrer during the irradiation experiments. The solution concentrations ranged from 0 to 0.28 M. The errors for the concentration measurements were approximately 2%–10%, which were caused by uncertainty of the weight measurement of the ascorbic acid using an electronic scale and volume measurement of water using a measuring cylinder.

3. Results and discussion

Figure 2 displays typical TOF mass spectra for positively charged ions emitted from pure water and an ascorbic acid solution with concentration of 55 μM upon 4.0-MeV C^{2+} ion bombardment. The vertical scale denotes the secondary ion intensity which is normalized to the total number of incident ions obtained by collecting the total beam current on the beam collimation slit during measurement of the TOF spectrum. The observed secondary ion species are H^+ and H_2O^+ ions originating from ionization and dissociation of water molecules, H_3O^+ formed by radiolysis involving an ion–molecule reaction in the physicochemical stage,

and protonated water cluster ions of $(H_2O)_{n-1}H_3O^+$ (n=2, 3, …). The cluster ions may be formed by aggregation of water molecules with H_3O^+ as a nucleus. Comparing the two targets, the TOF spectra are different in terms of spectral pattern (emitted secondary ion species), peak intensity and peak position. For instance, for the ascorbic acid solution target, the peaks consistent with the cluster ions were not observed within the experimental uncertainty. In addition, the peak intensity of H_3O^+ is clearly lower than that for the pure water target. These results imply that ascorbic acid prevented the formation of H_3O^+. Moreover, the peak positions of all the secondary ions (H^+, H_2O^+ and H_3O^+ ions) are shifted to longer flight times compared with those for the pure water target, and the profile of these peaks exhibits a tail toward longer flight times.

This peak shift may be attributed to decrease of electric field in the extraction region of the TOF spectrometer. In Figure 3, careful observation of the peak shift shows that its magnitude depends on ascorbic acid concentration. The vertical scale denotes the electric field acting to decelerate secondary ions, which is estimated from the flight-time delay corresponding to the peak shift. The upper horizontal scale denotes the pH corresponding to ascorbic acid concentration. The deceleration electric field increases with ascorbic acid concentration. The factor that the deceleration electric field produces may be related to ascorbic acid ($C_6H_8O_6$) being a weak electrolyte. In aqueous solution, ascorbic acid ionizes to form ascorbate ion, $C_6H_7O_6^-$.

We propose the following mechanism for secondary ion emission from liquid surfaces, in which we assume that ion emission is influenced by the surface charge of liquid materials. In aqueous solutions, surface charge is induced when solvent molecules in solutions (cations and anions) are distributed on surfaces with different concentrations. As a consequence of this surface charge, the emission of positive secondary ions increases for a positively charged surface because of the high surface concentrations of solute cations caused by Coulomb repulsion between these ions and the surface. Conversely, the positive ion emission is suppressed for a negatively charged surface because of the higher surface concentrations of solute anions. Thus, the secondary ion emission is influenced by charge polarity on the surface.

The following two reactions occur in aqueous solutions of ascorbic acid during irradiation: (1) acid dissociation of ascorbic acid, and (2) radical scavenger reaction of ascorbic acid. In reaction (1) (hereafter referred to as R1), the chemical equilibrium equation is given by

$$\mathrm{AsA\ (C_6H_8O_6) + H_2O \leftrightharpoons AsA^- + H_3O^+}\ , \qquad \text{(R1)}$$

where the equilibrium constant , pK_{a1}, is 4.25 [7]. Reaction (2) (hereafter referred to as R2) involves the reaction of two ascorbic acid molecules react with one OH· to produce one ascorbic acid ion (AsA^-) and one dehydroascorbate (DHA) molecule [8]:

$$\mathrm{2AsA + OH\cdot \rightarrow AsA^- + DHA}\ , \qquad \text{(R2)}$$

where one ascorbic acid molecule reacts with OH· as an antioxidant. In this work, R2 is used

as a scavenger reaction. In each chemical reaction, the concentration of AsA^- or H_3O^+ depends on the concentration of ascorbic acid.

We focus on the emission processes of secondary ion H_3O^+ from surfaces of ascorbic acid solution target. In the framework of water radiolysis, H_3O^+ is known to form pairs with OH· *via* an ion–molecule reaction: $H_2O^+ + H_2O \rightarrow H_3O^+ + OH\cdot$, where H_2O^+ is formed through ionization of water molecules by ionizing radiation [1]. Therefore, the behavior of H_3O^+ provides information about the effects of OH· radicals on reactions in aqueous solutions. To investigate the influence of interactions with AsA^- anions or H_3O^+ cations formed in R1 and R2 on H_3O^+ secondary ion emission, we measured the yield of H_3O^+ for different ascorbic acid concentrations by TOF mass spectrometry. The results are provided in Fig. 4, where the vertical scale represents the integrated peak intensity of H_3O^+ in the TOF spectra which is normalized to the total number of incident ions. One can see that the yield of H_3O^+ decreases considerably with increasing ascorbic acid concentration to approximately 60 μM, and then is saturated at high concentration. Similarly, the yield of protonated water cluster ions ($[H_2O]_{n-1}H_3O^+$) decreases with increasing ascorbic acid concentration. No cluster formation was observed above approximately 60 μM (not shown in this figure). These results suggest that solute cations and anoints described above strongly affects the ion emission of H_3O^+. To quantitatively estimate the observed results, we propose the following model of simple chemical equilibria. In this model, we assume that the secondary ion yield of H_3O^+ is

proportional to the surface concentrations of both H_3O^+ and AsA^- formed in R1 and R2. The secondary ion yield of H_3O^+, Y is given by

$$Y = Y_0 - \alpha([AsA^-]_{R1} - [H_3O^+]_{R1} + [AsA^-]_{R2}), \quad (1)$$

where Y_0 is the H_3O^+ yield of pure water, α is a constant, $[AsA^-]_{R1}$ and $[H_3O^+]_{R1}$ are the surface concentrations of AsA^- and H_3O^+ formed in R1, respectively, and $[AsA^-]_{R2}$ is the surface concentration of AsA^- formed in R2. The values of $[AsA^-]_{R1}$ and $[AsA^-]_{R2}$ increase with ascorbic acid concentration. In Eq. (1), the negative sing of $[AsA^-]_{R1}$ or $[AsA^-]_{R2}$ indicates suppression of the secondary ion emission of H_3O^+, whereas the positive sing of indicates enhancement of the secondary ion emission of H_3O^+.

According to Enami *et al*. [9], the surface concentration of H_3O^+ in an aqueous solution depends on pH. The surface concentration of H_3O^+ is extremely low above pH 4, but below pH 4 it becomes high. Based on this result, the observed emission yield of H_3O^+ depends on the pH of the ascorbic acid solutions. Figure 5 (a) reveals that the H_3O^+ yield decreased with increasing ascorbic acid concentrations in region I (pH > 4), and increased in region II (pH < 4). Moreover, the H_3O^+ yield is saturated at low pH (region III). A similar tendency is observed for the dependence of ascorbic acid concentration or pH on the peak shift in the TOF spectra shown in Fig. 3: at pH > 4 the deceleration electric field corresponding to the peak shift increases with ascorbic acid concentration, and becomes constant at pH < 4. These results suggest that when pH > 4, the surface of the aqueous solution is negatively charged

because of the presence of AsA^- formed in R1 and R2. Conversely, when pH < 4, the negative charge at the surface of the aqueous solution is lessened by an increase in the surface concentration of H_3O^+ formed in R1 (the $[H_3O^+]_{R1}$ value).

The observed pH dependence indicates that: (1) there is an upper concentration limit of ascorbic acid that has a radical scavenger effect, and (2) H_3O^+ and AsA^- concentrations in R1 are the same in the region in which the H_3O^+ yield is saturated. From these results, the H_3O^+ secondary ion yield for each region is given by the following three equations:

Region I: $$Y = Y_0 - \alpha([\mathrm{AsA^-}]_{R1} + [\mathrm{AsA^-}]_{R2}), \quad (2)$$

Region II: $$Y = Y_0 - \alpha([\mathrm{AsA^-}]_{R1} - [\mathrm{H_3O^+}]_{R1} + [\mathrm{AsA^-}]_{R2}), \quad (3)$$

Region III: $$Y = Y_0 - \alpha[\mathrm{AsA^-}]_{R2}, \quad (4)$$

where the values of $[AsA^-]_{R1}$, $[H_3O^+]_{R1}$, and $[AsA^-]_{R2}$ can be expressed as a function of ascorbic acid concentration, $[AsA]_{sol}$. The ion concentrations of AsA^- and H_3O^+ at the gas/liquid interface can be given as a function of those in the liquid bulk by the Langmuir adsorption model. According to this model, the values of $[AsA^-]_{R1}$ and $[H_3O^+]_{R1}$ are given by the following relations:

$$[\mathrm{AsA^-}]_{R1} = (K_{\mathrm{ASA^-}} W_{\mathrm{AsA^-}} [\mathrm{AsA^-}]_{bulk})/(1 + K_{\mathrm{AsA^-}} [\mathrm{AsA^-}]_{bulk}),$$

$$[\mathrm{H_3O^+}]_{R1} = \left(K_{\mathrm{H_3O^+}} W_{\mathrm{H_3O^+}} [\mathrm{H_3O^+}]_{bulk}\right)/\left(1 + K_{\mathrm{H_3O^+}} [\mathrm{H_3O^+}]_{bulk}\right),$$

where $[AsA^-]_{bulk}$ and $[H_3O^+]_{bulk}$ are the concentrations of AsA^- and H_3O^+ from R1 in the

liquid bulk, respectively, $K_{\mathrm{AsA^-}}$ and $K_{\mathrm{H_3O^+}}$ are equilibrium constants of AsA^- and H_3O^+ in the adsorption equilibrium state, respectively, and $W_{\mathrm{AsA^-}}$ and $W_{\mathrm{H_3O^+}}$ are the saturated concentrations of AsA^- and H_3O^+ from R1, respectively. Moreover, an ascorbic acid solution in an equilibrium state displays the following relations:

$$\mathrm{K_{a1}} = ([\mathrm{AsA^-}]_{\mathrm{bulk}}[\mathrm{H_3O^+}]_{\mathrm{bulk}})/[\mathrm{AsA}]_{\mathrm{bulk}},$$

$$[\mathrm{AsA^-}]_{\mathrm{bulk}} = [\mathrm{H_3O^+}]_{\mathrm{bulk}},$$

$$[\mathrm{AsA}]_{\mathrm{bulk}} = [\mathrm{AsA}]_{\mathrm{sol}} - [\mathrm{H_3O^+}]_{\mathrm{bulk}},$$

$$[\mathrm{AsA^-}]_{\mathrm{bulk}} = \left(-K_{\mathrm{a1}} + \sqrt{K_{\mathrm{a1}}^2 + 4K_{\mathrm{a1}}[\mathrm{AsA}]_{\mathrm{sol}}}\right)/2,$$

where K_{a1} is the equilibrium constant for R1, and $[AsA]_{bulk}$ is the concentration of AsA in the liquid bulk. As mentioned above, in R2, two AsA molecules react with one OH· to form one AsA^-. Therefore, the concentration of AsA^- from R2 at the liquid surface is given by $[\mathrm{AsA^-}]_{\mathrm{R2}} = [\mathrm{AsA}]_{\mathrm{bulk}}/2$. By taking into account these relations, the H_3O^+ secondary ion yield (Y in Eqs. (2) – (4)) can be expressed as a function of $[AsA]_{sol}$. In Fig. 5 (a), the model calculation using the fitting parameters $\alpha = 2 \times 10^4$, $K_{\mathrm{AsA^-}} = 4 \times 10^4\ \mathrm{M^{-1}}$, $K_{\mathrm{H_3O^+}} = 8 \times 10^4\ \mathrm{M^{-1}}$, and $W_{\mathrm{AsA^-}} = W_{\mathrm{H_3O^+}} = 2.5 \times 10^{-5}$ M, is shown as a solid line. In Fig. 5 (b) we present each calculation result of the dependence of H_3O^+ secondary ion yield on three types of surface concentrations $[AsA^-]_{R1}$, $[H_3O^+]_{R1}$ and $[AsA^-]_{R2}$. This model calculation is in good agreement with the experimental results.

In region III, the H_3O^+ ion emission yield only depends on $[AsA^-]_{R2}$. Therefore, we can

obtain the following relation: $-\alpha[\mathrm{AsA}^-]_{\mathrm{R2}} \geq Y_{\mathrm{sat}} - Y_0$, where Y_{sat} is the saturated yield of H_3O^+ in region III. By using this relation, the upper concentration limit of ascorbic acid acting as a radical scavenger is estimated to be approximately 70 μM (see Fig. 5). Interestingly, this value is comparable with the concentration of ascorbic acid in the blood (about 60 to 200 μM) [10]. This indicates that the ascorbic acid concentration in blood is sufficient to react with the total amount of OH· produced under the present irradiation conditions when all components of the human body are assumed to be water. Moreover, according to Hata *et al*. [11], ascorbic acid markedly lowered the yield of single-strand breaks of plasmid DNA irradiated by γ-rays to about 16% at an ascorbic acid concentration of 100 μM, and then gradually lowered the yield further to about 3% at an ascorbic acid concentration of 1000 μM. These results highlight the scavenger effect of ascorbic acid in a biological setting. From these comparisons, we conclude that the present results are useful for the study of scavenger effects observed in biological system.

4. Conclusion

We investigated the effects of a radical scavenger on radiolysis of aqueous solutions exposed to fast heavy-ion irradiation. Secondary ions emitted from aqueous solutions of ascorbic acid of different concentrations were measured using the vacuum liquid microjet technique. We determined the emission yield of H_3O^+ that forms in pairs with OH·, and its dependence on

ascorbic acid concentrations. By developing a model of the chemical equilibria in the solutions, the emission yield of H_3O^+ was estimated as a function of ascorbic acid concentration. In this model, the effect of the surface charge of the solutions was considered. The model calculation was in good agreement with the experimental results. We determined the upper concentration limit of ascorbic acid that acted as a radical scavenger was approximately 70 μM, which is comparable with the level of ascorbic acid in the blood. The present results may be applicable to studies of the effects of radical scavengers on biological systems.

Acknowledgments

We thank Makoto Imai and Manabu Saito of Kyoto University for valuable discussions. We also thank Masahiro Naitoh and Yoshitaka Sasaki of the accelerator facility of Quantum Science and Engineering Center, Kyoto University for their technical assistance during the experiments. This work was supported by Japan Society for the Promotion of Science (JSPS) Grants-in-Aid for Scientific Research (B) (Grant No. 19360427), and the Kyoto University Foundation.

References

[1] See, for example, G. R. Choppin, J. O. Liljenzin, and J. Rydberg, Radiochemistry and Nuclear Chemistry, 3rd ed. (Burlington, MA, 2002).

[2] M. Faubel, S. Schlemmer, and J. P. Toennies, Z. Phys. D 10 (1988) 269-277.

[3] F. Mafuné, J. Kohno, and T. Kondow. J. Phys. Chem. 100 (1996) 10041-10045.

[4] M. Kaneda, S. Sato, M. Shimizu, Z. He, K. Ishii, H. Tsuchida, and A. Itoh, Nucl. Instrum. Methods B 256 (2007) 97-100.

[5] T. Nebiki, T. Yamamoto, T. Narusawa, M. B. H. Breese, E. J. Teo, and F. Watt, J. Vac. Sci. Technol. A, 21 (2003) 1671.

[6] W. C. Wiley and I. H. McLaren, Rev. Sci. Instrum., 26 (1955) 1150-1157.

[7] B. Zümreoglu-Karan, Coor. Chem. Rev. 250 (2006) 2295-2307.

[8] B. H. J. Bielski, A. O. Allen, and H. A. Schwarz, J. Am. Chem. Soc. 103 (1981) 3516-3518.

[9] S. Enami, M. R. Hoffmann, and A. J. Colussi, J. Phys. Chem. Lett. 1 (2010) 1599-1604.

[10] M. J. González, J. R. Miranda-Massari, E. M. Mora, A. Guzmán, N. H. Riordan, H. D. Riordan, J. J. Casciari, J. A. Jackson, and A. Román-Franco, Integr. Cancer Ther. 4 (2005) 32.

[11] K. Hata, A. Urushibara, S. Yamashita, N. Shikazono, A. Yokoya, and Y. Katsumura, Biochem. Biophys. Res. Commun., 434 (2013) 341-345.

Figure captions

Fig. 1. Schematic diagram of the experimental setup for measurement of ion-induced secondary ion emission from a liquid microjet target under vacuum; (a) Photograph of the pin-point irradiation of a liquid jet target by an ion microbeam produced using a capillary beam-focusing method. The black circle in the background denotes the entrance orifice of the flight tube. (b) Schematic diagram of the ion irradiation area.

Fig. 2. TOF mass spectra of positively charged secondary ions emitted from (a) pure water and (b) aqueous ascorbic acid solution with a concentration of 55 μM by 4.0-MeV C^{2+} ion bombardment. The vertical scale indicates the ion intensity normalized by the total number of incident ions.

Fig. 3. Estimated deceleration electric fields from the peak shifts in the TOF mass spectra as a function of ascorbic acid concentration (or the corresponding pH). The filled and open circles denote experimental data for H^+ and H_3O^+secondary ions, respectively. The dashed line is a visual guide.

Fig. 4. Dependence of H_3O^+ secondary ion yield on ascorbic acid concentration (or the corresponding pH). The vertical scale denotes the integrated peak intensity of H_3O^+ in the TOF spectra.

Fig. 5. (a) Comparison of experimental results and model calculations for the dependence of H_3O^+ secondary ion yield on ascorbic acid concentration up to 1200 μM (or the corresponding

pH). The black line shows the fitting curve obtained from the present model. (b) Model calculations for the dependence of H_3O^+ emission rate on ascorbic acid concentrations. Green curve: suppression effect of H_3O^+ emission due to solute anions AsA^- produced in R1, red curve: radical scavenger effect caused by solute anions AsA^- produced in R2, and blue curve: additional production caused by solute cations H_3O^+ produced in R2.

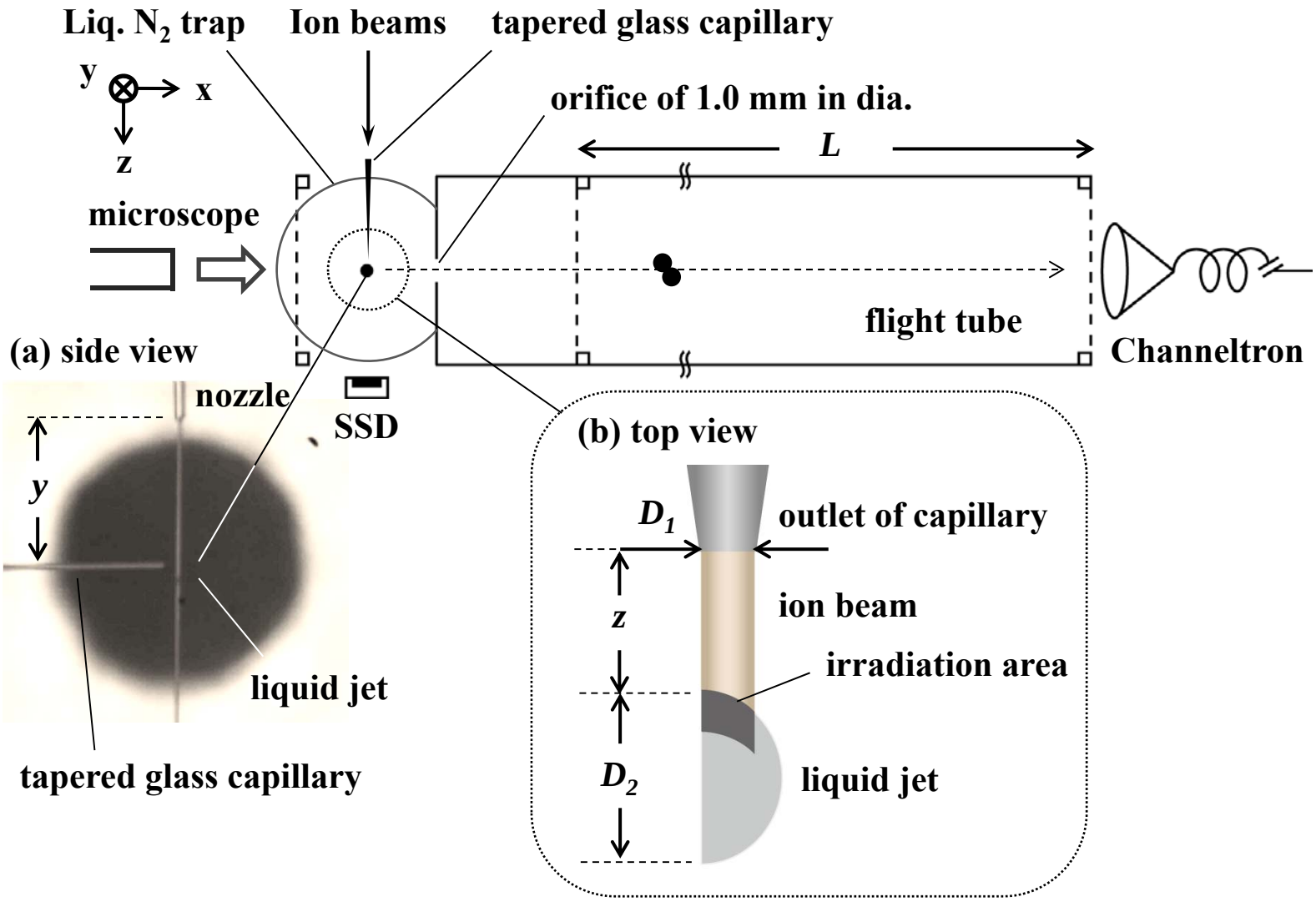

Figure 1 Nomura *et al.*

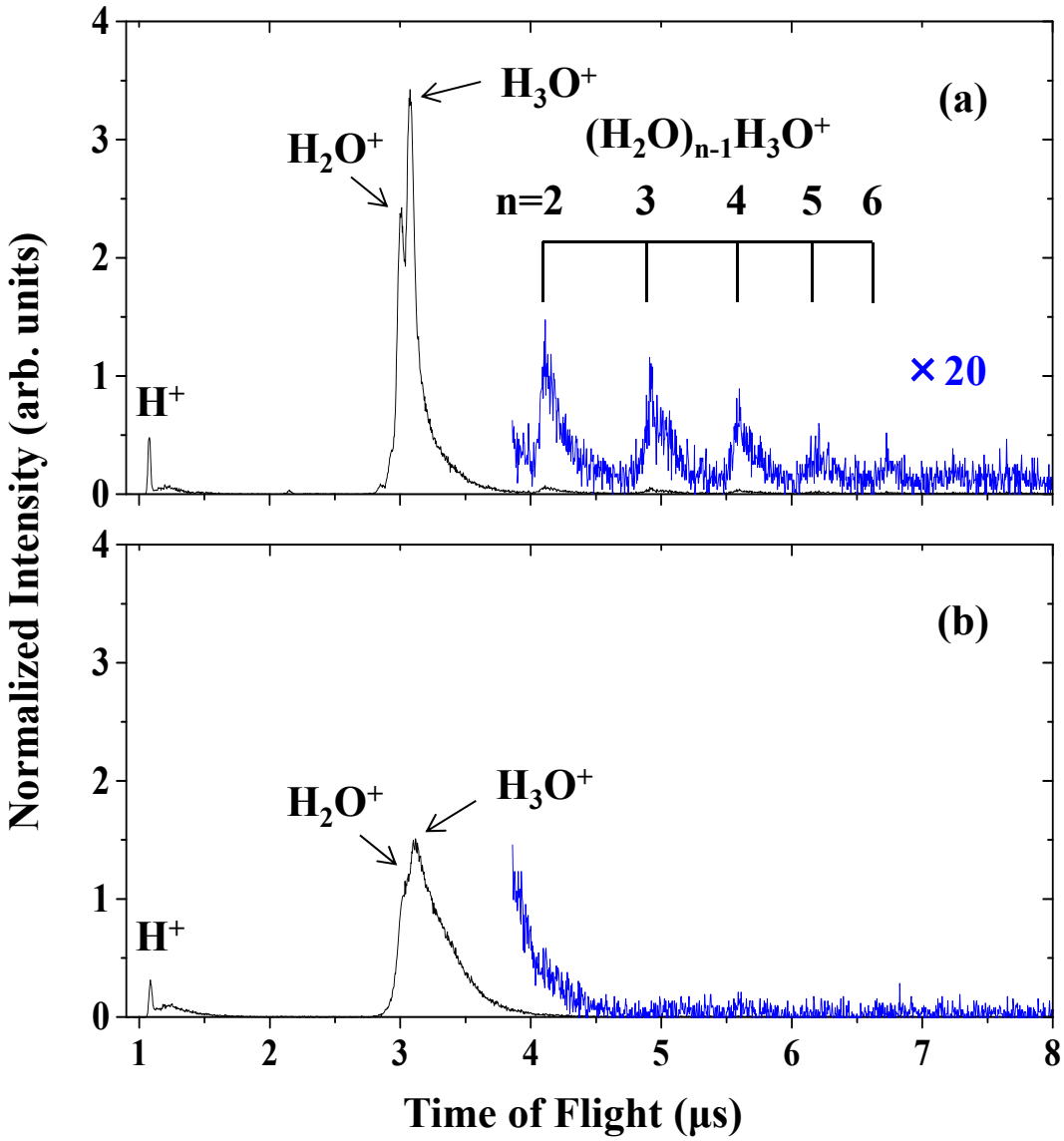

Figure 2 Nomura *et al.*

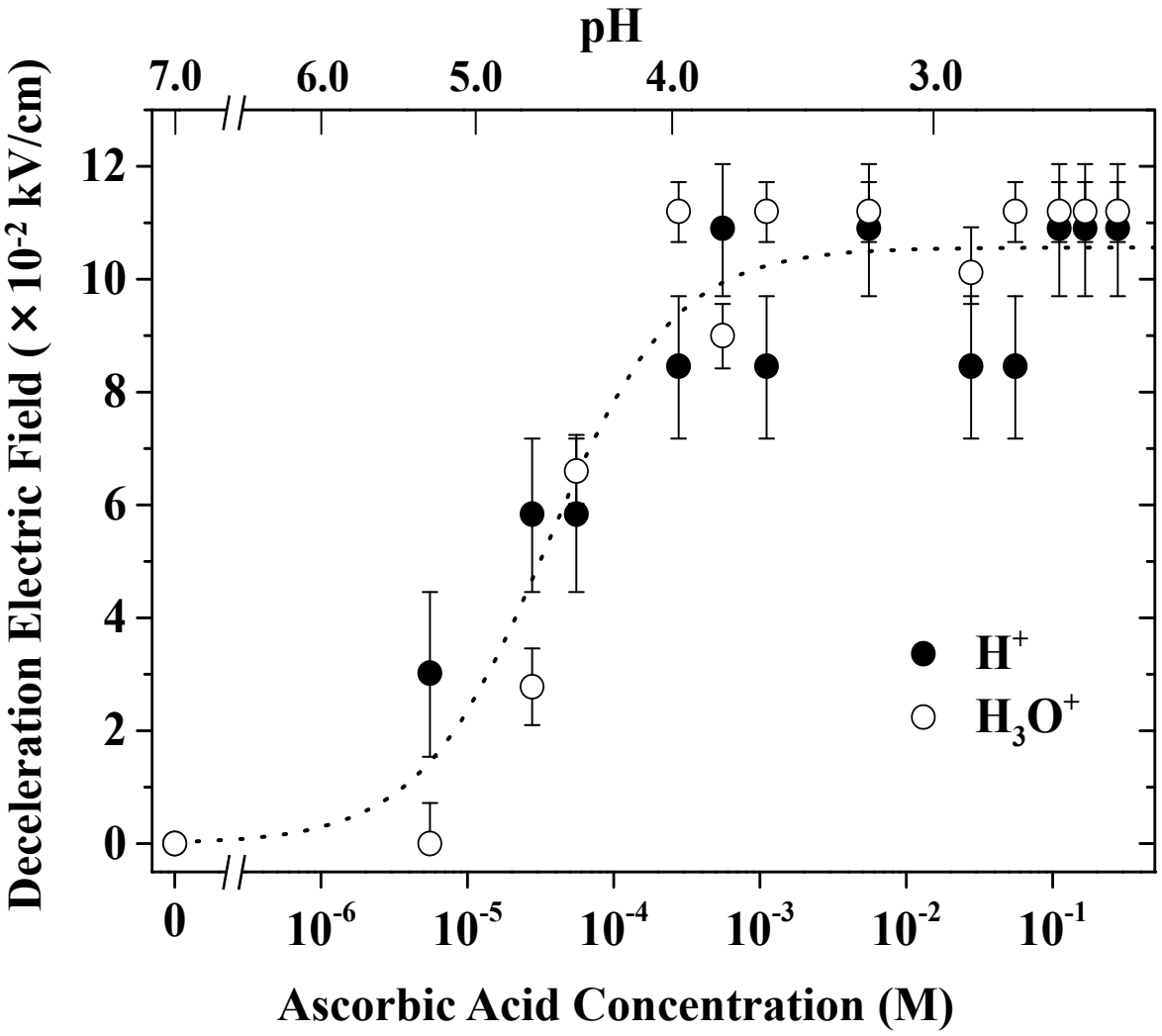

Figure 3 Nomura *et al.*

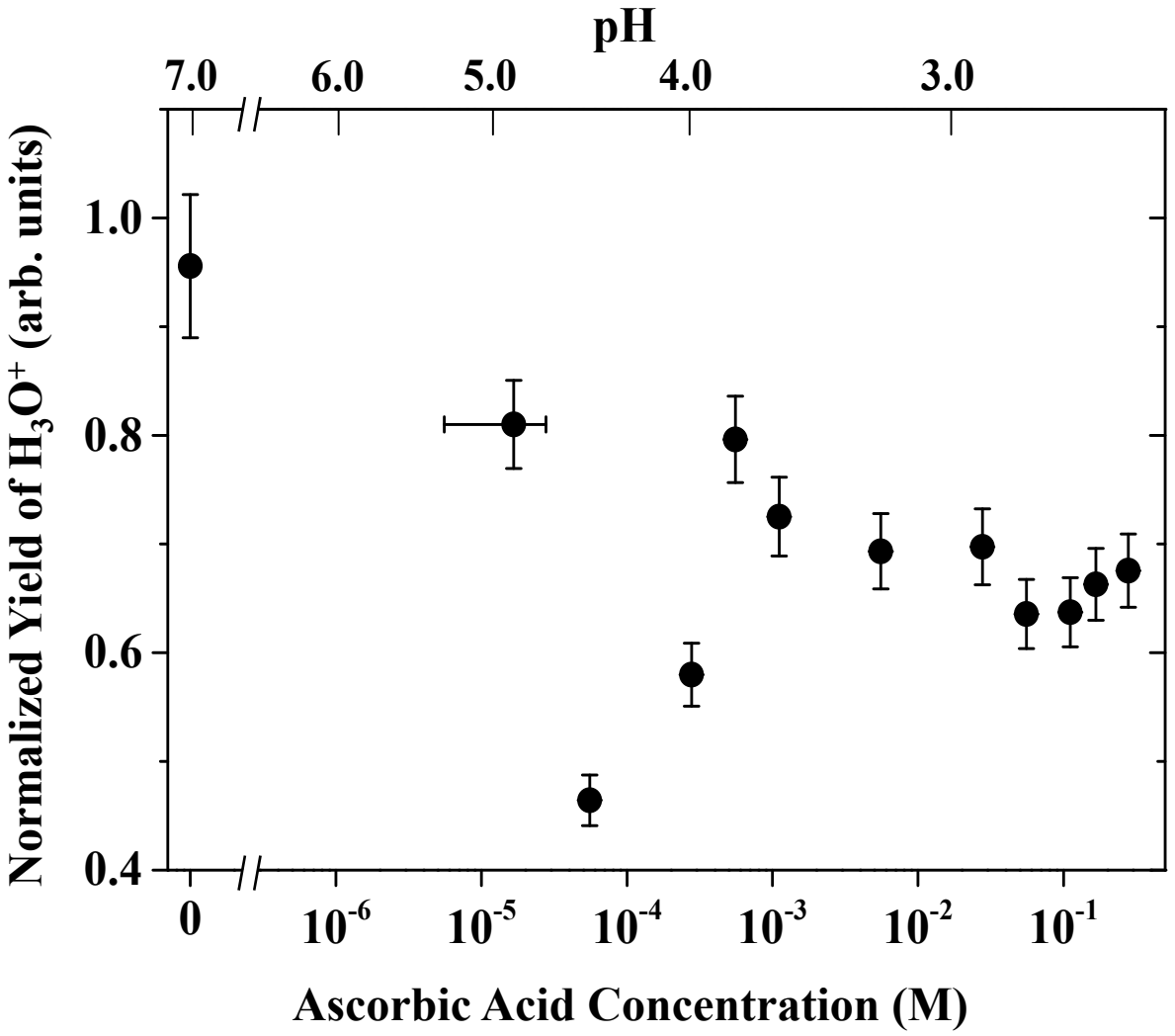

Figure 4 Nomura *et al.*

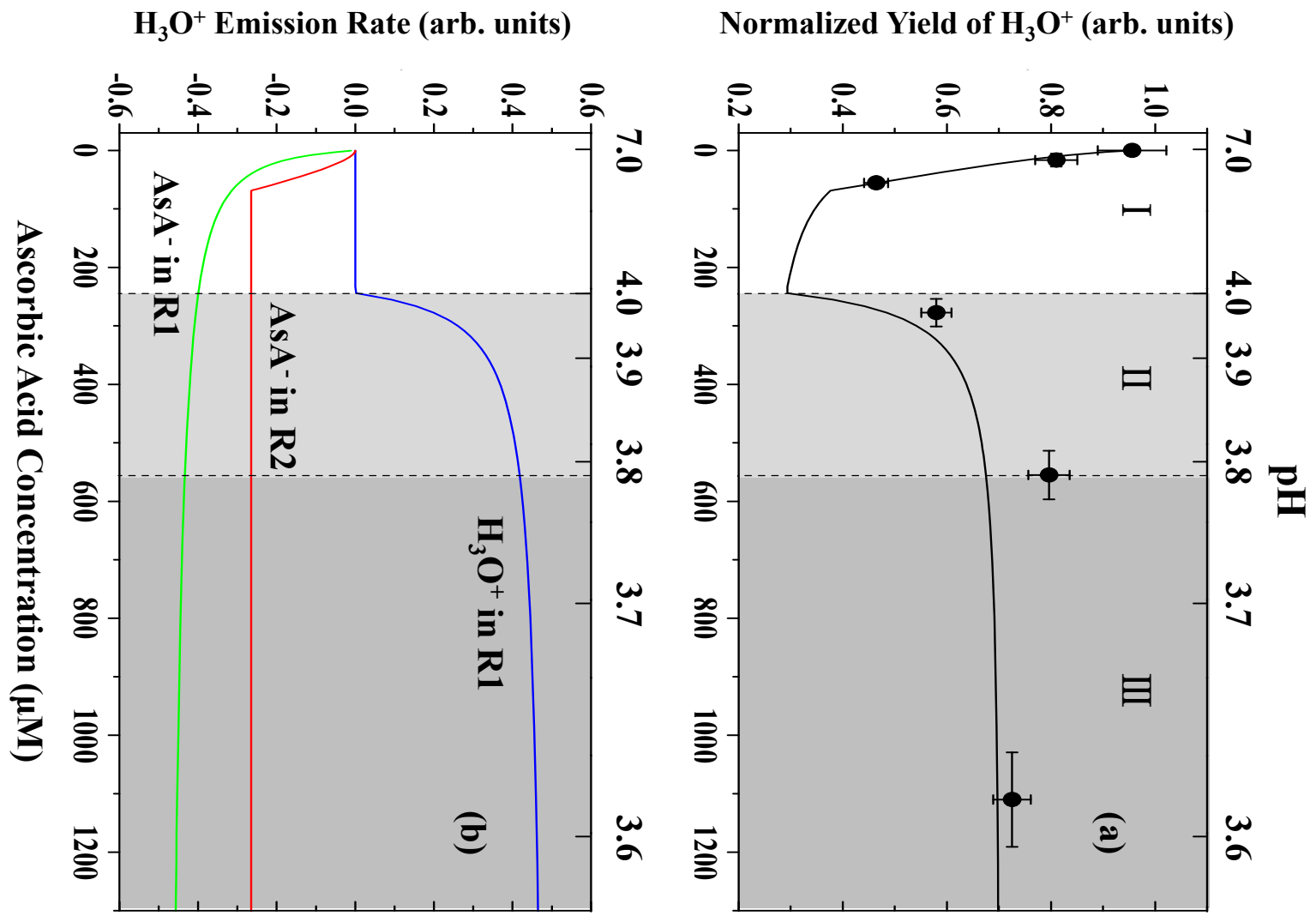

Figure 5 Nomura *et al.*